

Cosmic rays and galactic dust: maverick-style

Philipp Mertsch

SubirFest2023, Oxford
13 September 2023

Where it all started



October 2007

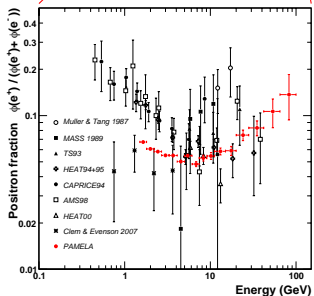


PAMELA

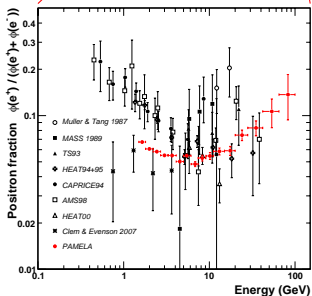
In August 2008, a man took a photograph
somewhere in Stockholm . . .



In August 2008, a man took a photograph somewhere in Stockholm . . .



In August 2008, a man took a photograph somewhere in Stockholm . . .



LETTERS

An anomalous positron abundance in cosmic rays with energies 1.5–100 GeV

O. Adriani^{1,2}, G. C. Barbarino^{1,4}, G. A. Bazilevskaya³, R. Bellotti^{1,2}, M. Boezio^{1,5}, E. A. Bogomolov⁶, L. Bonechi^{1,2}, M. Bongi¹, V. Bonvicini⁶, S. Bottai¹, A. Bruno^{1,2}, F. Cafagna¹, D. Campana¹, P. Carlson¹⁰, M. Casolino¹¹, G. Castellini¹¹, M. P. De Pascale^{1,12}, G. De Rosa¹, N. De Simone^{1,13}, V. Di Felice^{1,14}, A. M. Galper¹⁵, L. Grishantseva¹⁶, P. Hofverberg¹⁷, S. V. Koldashov³, S. Y. Krut'kov³, A. N. Kvashnin³, A. Leonov¹⁸, V. Malvezzi¹⁹, L. Marcellini¹⁹, W. Menz¹⁹, V. V. Mikhailov¹⁹, E. Micchietti²⁰, S. Orsi²¹, G. Osteria²², P. Papini²³, M. Pearce²⁴, P. Picot²⁵, M. Ricci¹, S. B. Ricciarini¹, M. Simon¹⁰, R. Sparvoli^{11,12}, P. Spillantini^{1,2}, Y. I. Stozhkov⁶, A. Vacchi¹, E. Vannucini¹, G. Vasilyev⁶, S. A. Voronov¹¹, Y. T. Yurkin¹¹, G. Zampà¹, N. Zampa¹ & V. G. Zverev¹⁴

Antiparticles account for a small fraction of cosmic rays and are known to be produced in interactions between cosmic-ray nuclei and atoms in the interstellar medium, which is referred to as a 'secondary source'. Positrons might also originate in objects such as pulsars¹ and microquasars² or through dark matter annihilation³, which would be 'primary sources'. Previous statistically limited measurements^{4–10} of the ratio of positron and electron fluxes have been interpreted as evidence for a primary source for the positrons, as has an increase in the total electron+positron flux at energies between 300 and 400 GeV (ref. 8). Here we report a measurement of the positron fraction in the energy range 1.5–100 GeV. We find that the positron fraction increases sharply over much of that range, in a way that appears to be completely inconsistent with secondary sources. We therefore conclude that a primary source, be it an astrophysical object or dark matter annihilation, is necessary.

The results presented here are based on the data we collected by the PAMELA satellite-borne experiment¹¹ between July 2006 and February 2008. More than 10⁷ protons were accumulated during a total acquisition time of approximately 500 days. From these triggered events, 151,672 electrons and 9,450 positrons were identified in the energy interval 1.5–100 GeV. Results are presented as a positron fraction—that is, the ratio of positron flux to the sum of electron and positron fluxes, $\phi(e^+)/[\phi(e^-)+\phi(e^+)]$ —and are shown in Table 1. The apparatus is a system of electronic particle detectors optimized for the study of antiparticles in the cosmic radiation (Supplementary Information section 1). It was launched from the Bajkonur cosmodrome on 13 June 2006 on the Russian satellite for space physics 'Fobos' (information only), at an altitude varying between 350 km and 610 km. A permanent magnet spectrometer with a silicon tracking system allows the rigidity (momentum/charge, coded in units of GV), and sign-of-charge of the incident particle to be determined. The interaction pattern in an imaging silicon-tungsten calorimeter allows electron and positrons to be separated from protons.

The identification of protons is the largest source of background when estimating the positron fraction. This can occur if electron and proton-like interaction patterns are confused in the calorimeter. This would lead to Fig. 2 showing a calculation based on

calorimeter data. The proton-to-positron flux ratio increases from approximately 10¹ at 1 GV to approximately 10⁴ at 100 GV. Robust proton identification is therefore required, and the residual proton background must be estimated accurately. The imaging calorimeter is 16.3 radiation lengths (16.8 nuclear interaction lengths) deep, so electron and positron decay will contain electromagnetic showers in the energy range of interest. In contrast, the majority of the protons will either pass through the calorimeter as minimum ionizing particles or interact deep in the calorimeter.

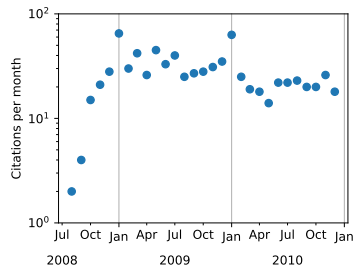
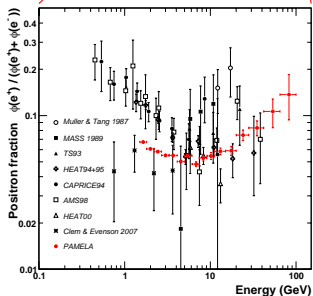
This is illustrated in Fig. 1, which shows Z , the fraction of calorimeter energy deposited inside a cylinder of radius 0.5 Moliere radii, as a function of deflection (rigidity)¹². The axis of the cylinder is defined by extrapolating the particle track reconstructed in the spectrometer. For negatively-signed deflections, electrons are clearly visible as a horizontal band with Z lying mostly between 0.4 and 0.7. For positively-signed deflections, the similar horizontal band is naturally associated with positrons, with the remaining proton, mostly at $Z < 0.4$, designated as a proton contamination (see Supplementary Information sections 2 and 3 for additional details concerning particle selection and background determination).

Figure 2 shows the positron fraction measured by the PAMELA experiment compared with other recent experimental data. The PAMELA data covers the energy range 1.5–100 GeV, with significantly higher statistics than other measurements. Two features are clearly visible in the data. At low energies (below 5 GeV) the PAMELA results are systematically lower than data collected during the 1990s, and at high energies (above 10 GeV) the PAMELA results show that the positron fraction increases significantly with energy.

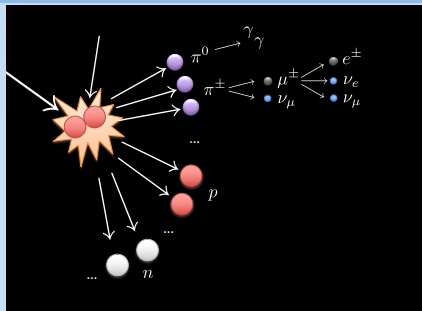
Measurements of cosmic-ray positrons and electrons address a number of questions in contemporary astrophysics, such as the nature and distribution of particle sources in our Galaxy, and the subsequent propagation of cosmic rays through the Galaxy and the solar heliosphere. Positrons are believed to be mostly created in secondary production processes, that is, by the interaction of cosmic-ray nuclei with the interstellar gas. This would lead to Fig. 2 showing a calculation based on

¹University of Ferrara, Department of Physics, Via Giuseppe I. 1-40129 Sesto Cavallotti, Ferrara, Italy; ²INFN, Sezione di Ferrara, Via Saraceno 1, 40129 Sesto Cavallotti, Ferrara, Italy; ³Tomsk State University, 630012 Tomsk, Russia; ⁴INFN, Sezione di Padova, Via Marzotto 1, 35100 Padova, Italy; ⁵INFN, Sezione di Bologna, Via Irace 1, 40139 Bologna, Italy; ⁶INFN, Sezione di Bari, Via Amendola 173, 70126 Bari, Italy; ⁷INFN, Sezione di Roma, Via Ardeatina 546, 00187 Roma, Italy; ⁸INFN, Sezione di Trieste, Via Strada 6, 34100 Trieste, Italy; ⁹INFN, Sezione di Genova, Via Dodecaneso 33, 16146 Genova, Italy; ¹⁰INFN, Sezione di Pisa, Via F. Strozzi 2, 56127 Pisa, Italy; ¹¹INFN, Sezione di Roma, Via Ardeatina 546, 00187 Roma, Italy; ¹²INFN, Sezione di Padova, Via Marzotto 1, 35100 Padova, Italy; ¹³INFN, Sezione di Bologna, Via Irace 1, 40139 Bologna, Italy; ¹⁴INFN, Sezione di Bari, Via Amendola 173, 70126 Bari, Italy; ¹⁵INFN, Sezione di Roma, Via Ardeatina 546, 00187 Roma, Italy; ¹⁶INFN, Sezione di Trieste, Via Strada 6, 34100 Trieste, Italy; ¹⁷INFN, Sezione di Genova, Via Dodecaneso 33, 16146 Genova, Italy; ¹⁸INFN, Sezione di Pisa, Via F. Strozzi 2, 56127 Pisa, Italy; ¹⁹INFN, Sezione di Roma, Via Ardeatina 546, 00187 Roma, Italy; ²⁰INFN, Sezione di Padova, Via Marzotto 1, 35100 Padova, Italy; ²¹INFN, Sezione di Bologna, Via Irace 1, 40139 Bologna, Italy; ²²INFN, Sezione di Bari, Via Amendola 173, 70126 Bari, Italy; ²³INFN, Sezione di Roma, Via Ardeatina 546, 00187 Roma, Italy; ²⁴INFN, Sezione di Trieste, Via Strada 6, 34100 Trieste, Italy; ²⁵INFN, Sezione di Genova, Via Dodecaneso 33, 16146 Genova, Italy; ²⁶INFN, Sezione di Pisa, Via F. Strozzi 2, 56127 Pisa, Italy; ²⁷INFN, Sezione di Roma, Via Ardeatina 546, 00187 Roma, Italy; ²⁸INFN, Sezione di Padova, Via Marzotto 1, 35100 Padova, Italy; ²⁹INFN, Sezione di Bologna, Via Irace 1, 40139 Bologna, Italy; ³⁰INFN, Sezione di Bari, Via Amendola 173, 70126 Bari, Italy; ³¹INFN, Sezione di Roma, Via Ardeatina 546, 00187 Roma, Italy; ³²INFN, Sezione di Trieste, Via Strada 6, 34100 Trieste, Italy; ³³INFN, Sezione di Genova, Via Dodecaneso 33, 16146 Genova, Italy; ³⁴INFN, Sezione di Pisa, Via F. Strozzi 2, 56127 Pisa, Italy; ³⁵INFN, Sezione di Roma, Via Ardeatina 546, 00187 Roma, Italy; ³⁶INFN, Sezione di Padova, Via Marzotto 1, 35100 Padova, Italy; ³⁷INFN, Sezione di Bologna, Via Irace 1, 40139 Bologna, Italy; ³⁸INFN, Sezione di Bari, Via Amendola 173, 70126 Bari, Italy; ³⁹INFN, Sezione di Roma, Via Ardeatina 546, 00187 Roma, Italy; ⁴⁰INFN, Sezione di Trieste, Via Strada 6, 34100 Trieste, Italy; ⁴¹INFN, Sezione di Genova, Via Dodecaneso 33, 16146 Genova, Italy; ⁴²INFN, Sezione di Pisa, Via F. Strozzi 2, 56127 Pisa, Italy; ⁴³INFN, Sezione di Roma, Via Ardeatina 546, 00187 Roma, Italy; ⁴⁴INFN, Sezione di Padova, Via Marzotto 1, 35100 Padova, Italy; ⁴⁵INFN, Sezione di Bologna, Via Irace 1, 40139 Bologna, Italy; ⁴⁶INFN, Sezione di Bari, Via Amendola 173, 70126 Bari, Italy; ⁴⁷INFN, Sezione di Roma, Via Ardeatina 546, 00187 Roma, Italy; ⁴⁸INFN, Sezione di Trieste, Via Strada 6, 34100 Trieste, Italy; ⁴⁹INFN, Sezione di Genova, Via Dodecaneso 33, 16146 Genova, Italy; ⁵⁰INFN, Sezione di Pisa, Via F. Strozzi 2, 56127 Pisa, Italy; ⁵¹INFN, Sezione di Roma, Via Ardeatina 546, 00187 Roma, Italy; ⁵²INFN, Sezione di Padova, Via Marzotto 1, 35100 Padova, Italy; ⁵³INFN, Sezione di Bologna, Via Irace 1, 40139 Bologna, Italy; ⁵⁴INFN, Sezione di Bari, Via Amendola 173, 70126 Bari, Italy; ⁵⁵INFN, Sezione di Roma, Via Ardeatina 546, 00187 Roma, Italy; ⁵⁶INFN, Sezione di Trieste, Via Strada 6, 34100 Trieste, Italy; ⁵⁷INFN, Sezione di Genova, Via Dodecaneso 33, 16146 Genova, Italy; ⁵⁸INFN, Sezione di Pisa, Via F. Strozzi 2, 56127 Pisa, Italy; ⁵⁹INFN, Sezione di Roma, Via Ardeatina 546, 00187 Roma, Italy; ⁶⁰INFN, Sezione di Padova, Via Marzotto 1, 35100 Padova, Italy; ⁶¹INFN, Sezione di Bologna, Via Irace 1, 40139 Bologna, Italy; ⁶²INFN, Sezione di Bari, Via Amendola 173, 70126 Bari, Italy; ⁶³INFN, Sezione di Roma, Via Ardeatina 546, 00187 Roma, Italy; ⁶⁴INFN, Sezione di Trieste, Via Strada 6, 34100 Trieste, Italy; ⁶⁵INFN, Sezione di Genova, Via Dodecaneso 33, 16146 Genova, Italy; ⁶⁶INFN, Sezione di Pisa, Via F. Strozzi 2, 56127 Pisa, Italy; ⁶⁷INFN, Sezione di Roma, Via Ardeatina 546, 00187 Roma, Italy; ⁶⁸INFN, Sezione di Padova, Via Marzotto 1, 35100 Padova, Italy; ⁶⁹INFN, Sezione di Bologna, Via Irace 1, 40139 Bologna, Italy; ⁷⁰INFN, Sezione di Bari, Via Amendola 173, 70126 Bari, Italy; ⁷¹INFN, Sezione di Roma, Via Ardeatina 546, 00187 Roma, Italy; ⁷²INFN, Sezione di Trieste, Via Strada 6, 34100 Trieste, Italy; ⁷³INFN, Sezione di Genova, Via Dodecaneso 33, 16146 Genova, Italy; ⁷⁴INFN, Sezione di Pisa, Via F. Strozzi 2, 56127 Pisa, Italy; ⁷⁵INFN, Sezione di Roma, Via Ardeatina 546, 00187 Roma, Italy; ⁷⁶INFN, Sezione di Padova, Via Marzotto 1, 35100 Padova, Italy; ⁷⁷INFN, Sezione di Bologna, Via Irace 1, 40139 Bologna, Italy; ⁷⁸INFN, Sezione di Bari, Via Amendola 173, 70126 Bari, Italy; ⁷⁹INFN, Sezione di Roma, Via Ardeatina 546, 00187 Roma, Italy; ⁸⁰INFN, Sezione di Trieste, Via Strada 6, 34100 Trieste, Italy; ⁸¹INFN, Sezione di Genova, Via Dodecaneso 33, 16146 Genova, Italy; ⁸²INFN, Sezione di Pisa, Via F. Strozzi 2, 56127 Pisa, Italy; ⁸³INFN, Sezione di Roma, Via Ardeatina 546, 00187 Roma, Italy; ⁸⁴INFN, Sezione di Padova, Via Marzotto 1, 35100 Padova, Italy; ⁸⁵INFN, Sezione di Bologna, Via Irace 1, 40139 Bologna, Italy; ⁸⁶INFN, Sezione di Bari, Via Amendola 173, 70126 Bari, Italy; ⁸⁷INFN, Sezione di Roma, Via Ardeatina 546, 00187 Roma, Italy; ⁸⁸INFN, Sezione di Trieste, Via Strada 6, 34100 Trieste, Italy; ⁸⁹INFN, Sezione di Genova, Via Dodecaneso 33, 16146 Genova, Italy; ⁹⁰INFN, Sezione di Pisa, Via F. Strozzi 2, 56127 Pisa, Italy; ⁹¹INFN, Sezione di Roma, Via Ardeatina 546, 00187 Roma, Italy; ⁹²INFN, Sezione di Padova, Via Marzotto 1, 35100 Padova, Italy; ⁹³INFN, Sezione di Bologna, Via Irace 1, 40139 Bologna, Italy; ⁹⁴INFN, Sezione di Bari, Via Amendola 173, 70126 Bari, Italy; ⁹⁵INFN, Sezione di Roma, Via Ardeatina 546, 00187 Roma, Italy; ⁹⁶INFN, Sezione di Trieste, Via Strada 6, 34100 Trieste, Italy; ⁹⁷INFN, Sezione di Genova, Via Dodecaneso 33, 16146 Genova, Italy; ⁹⁸INFN, Sezione di Pisa, Via F. Strozzi 2, 56127 Pisa, Italy; ⁹⁹INFN, Sezione di Roma, Via Ardeatina 546, 00187 Roma, Italy; ¹⁰⁰INFN, Sezione di Padova, Via Marzotto 1, 35100 Padova, Italy; ¹⁰¹INFN, Sezione di Bologna, Via Irace 1, 40139 Bologna, Italy; ¹⁰²INFN, Sezione di Bari, Via Amendola 173, 70126 Bari, Italy; ¹⁰³INFN, Sezione di Roma, Via Ardeatina 546, 00187 Roma, Italy; ¹⁰⁴INFN, Sezione di Trieste, Via Strada 6, 34100 Trieste, Italy; ¹⁰⁵INFN, Sezione di Genova, Via Dodecaneso 33, 16146 Genova, Italy; ¹⁰⁶INFN, Sezione di Pisa, Via F. Strozzi 2, 56127 Pisa, Italy; ¹⁰⁷INFN, Sezione di Roma, Via Ardeatina 546, 00187 Roma, Italy; ¹⁰⁸INFN, Sezione di Padova, Via Marzotto 1, 35100 Padova, Italy; ¹⁰⁹INFN, Sezione di Bologna, Via Irace 1, 40139 Bologna, Italy; ¹¹⁰INFN, Sezione di Bari, Via Amendola 173, 70126 Bari, Italy; ¹¹¹INFN, Sezione di Roma, Via Ardeatina 546, 00187 Roma, Italy; ¹¹²INFN, Sezione di Trieste, Via Strada 6, 34100 Trieste, Italy; ¹¹³INFN, Sezione di Genova, Via Dodecaneso 33, 16146 Genova, Italy; ¹¹⁴INFN, Sezione di Pisa, Via F. Strozzi 2, 56127 Pisa, Italy; ¹¹⁵INFN, Sezione di Roma, Via Ardeatina 546, 00187 Roma, Italy; ¹¹⁶INFN, Sezione di Padova, Via Marzotto 1, 35100 Padova, Italy; ¹¹⁷INFN, Sezione di Bologna, Via Irace 1, 40139 Bologna, Italy; ¹¹⁸INFN, Sezione di Bari, Via Amendola 173, 70126 Bari, Italy; ¹¹⁹INFN, Sezione di Roma, Via Ardeatina 546, 00187 Roma, Italy; ¹²⁰INFN, Sezione di Trieste, Via Strada 6, 34100 Trieste, Italy; ¹²¹INFN, Sezione di Genova, Via Dodecaneso 33, 16146 Genova, Italy; ¹²²INFN, Sezione di Pisa, Via F. Strozzi 2, 56127 Pisa, Italy; ¹²³INFN, Sezione di Roma, Via Ardeatina 546, 00187 Roma, Italy; ¹²⁴INFN, Sezione di Padova, Via Marzotto 1, 35100 Padova, Italy; ¹²⁵INFN, Sezione di Bologna, Via Irace 1, 40139 Bologna, Italy; ¹²⁶INFN, Sezione di Bari, Via Amendola 173, 70126 Bari, Italy; ¹²⁷INFN, Sezione di Roma, Via Ardeatina 546, 00187 Roma, Italy; ¹²⁸INFN, Sezione di Trieste, Via Strada 6, 34100 Trieste, Italy; ¹²⁹INFN, Sezione di Genova, Via Dodecaneso 33, 16146 Genova, Italy; ¹³⁰INFN, Sezione di Pisa, Via F. Strozzi 2, 56127 Pisa, Italy; ¹³¹INFN, Sezione di Roma, Via Ardeatina 546, 00187 Roma, Italy; ¹³²INFN, Sezione di Padova, Via Marzotto 1, 35100 Padova, Italy; ¹³³INFN, Sezione di Bologna, Via Irace 1, 40139 Bologna, Italy; ¹³⁴INFN, Sezione di Bari, Via Amendola 173, 70126 Bari, Italy; ¹³⁵INFN, Sezione di Roma, Via Ardeatina 546, 00187 Roma, Italy; ¹³⁶INFN, Sezione di Trieste, Via Strada 6, 34100 Trieste, Italy; ¹³⁷INFN, Sezione di Genova, Via Dodecaneso 33, 16146 Genova, Italy; ¹³⁸INFN, Sezione di Pisa, Via F. Strozzi 2, 56127 Pisa, Italy; ¹³⁹INFN, Sezione di Roma, Via Ardeatina 546, 00187 Roma, Italy; ¹⁴⁰INFN, Sezione di Padova, Via Marzotto 1, 35100 Padova, Italy; ¹⁴¹INFN, Sezione di Bologna, Via Irace 1, 40139 Bologna, Italy; ¹⁴²INFN, Sezione di Bari, Via Amendola 173, 70126 Bari, Italy; ¹⁴³INFN, Sezione di Roma, Via Ardeatina 546, 00187 Roma, Italy; ¹⁴⁴INFN, Sezione di Trieste, Via Strada 6, 34100 Trieste, Italy; ¹⁴⁵INFN, Sezione di Genova, Via Dodecaneso 33, 16146 Genova, Italy; ¹⁴⁶INFN, Sezione di Pisa, Via F. Strozzi 2, 56127 Pisa, Italy; ¹⁴⁷INFN, Sezione di Roma, Via Ardeatina 546, 00187 Roma, Italy; ¹⁴⁸INFN, Sezione di Padova, Via Marzotto 1, 35100 Padova, Italy; ¹⁴⁹INFN, Sezione di Bologna, Via Irace 1, 40139 Bologna, Italy; ¹⁵⁰INFN, Sezione di Bari, Via Amendola 173, 70126 Bari, Italy; ¹⁵¹INFN, Sezione di Roma, Via Ardeatina 546, 00187 Roma, Italy; ¹⁵²INFN, Sezione di Trieste, Via Strada 6, 34100 Trieste, Italy; ¹⁵³INFN, Sezione di Genova, Via Dodecaneso 33, 16146 Genova, Italy; ¹⁵⁴INFN, Sezione di Pisa, Via F. Strozzi 2, 56127 Pisa, Italy; ¹⁵⁵INFN, Sezione di Roma, Via Ardeatina 546, 00187 Roma, Italy; ¹⁵⁶INFN, Sezione di Padova, Via Marzotto 1, 35100 Padova, Italy; ¹⁵⁷INFN, Sezione di Bologna, Via Irace 1, 40139 Bologna, Italy; ¹⁵⁸INFN, Sezione di Bari, Via Amendola 173, 70126 Bari, Italy; ¹⁵⁹INFN, Sezione di Roma, Via Ardeatina 546, 00187 Roma, Italy; ¹⁶⁰INFN, Sezione di Trieste, Via Strada 6, 34100 Trieste, Italy; ¹⁶¹INFN, Sezione di Genova, Via Dodecaneso 33, 16146 Genova, Italy; ¹⁶²INFN, Sezione di Pisa, Via F. Strozzi 2, 56127 Pisa, Italy; ¹⁶³INFN, Sezione di Roma, Via Ardeatina 546, 00187 Roma, Italy; ¹⁶⁴INFN, Sezione di Padova, Via Marzotto 1, 35100 Padova, Italy; ¹⁶⁵INFN, Sezione di Bologna, Via Irace 1, 40139 Bologna, Italy; ¹⁶⁶INFN, Sezione di Bari, Via Amendola 173, 70126 Bari, Italy; ¹⁶⁷INFN, Sezione di Roma, Via Ardeatina 546, 00187 Roma, Italy; ¹⁶⁸INFN, Sezione di Trieste, Via Strada 6, 34100 Trieste, Italy; ¹⁶⁹INFN, Sezione di Genova, Via Dodecaneso 33, 16146 Genova, Italy; ¹⁷⁰INFN, Sezione di Pisa, Via F. Strozzi 2, 56127 Pisa, Italy; ¹⁷¹INFN, Sezione di Roma, Via Ardeatina 546, 00187 Roma, Italy; ¹⁷²INFN, Sezione di Padova, Via Marzotto 1, 35100 Padova, Italy; ¹⁷³INFN, Sezione di Bologna, Via Irace 1, 40139 Bologna, Italy; ¹⁷⁴INFN, Sezione di Bari, Via Amendola 173, 70126 Bari, Italy; ¹⁷⁵INFN, Sezione di Roma, Via Ardeatina 546, 00187 Roma, Italy; ¹⁷⁶INFN, Sezione di Trieste, Via Strada 6, 34100 Trieste, Italy; ¹⁷⁷INFN, Sezione di Genova, Via Dodecaneso 33, 16146 Genova, Italy; ¹⁷⁸INFN, Sezione di Pisa, Via F. Strozzi 2, 56127 Pisa, Italy; ¹⁷⁹INFN, Sezione di Roma, Via Ardeatina 546, 00187 Roma, Italy; ¹⁸⁰INFN, Sezione di Padova, Via Marzotto 1, 35100 Padova, Italy; ¹⁸¹INFN, Sezione di Bologna, Via Irace 1, 40139 Bologna, Italy; ¹⁸²INFN, Sezione di Bari, Via Amendola 173, 70126 Bari, Italy; ¹⁸³INFN, Sezione di Roma, Via Ardeatina 546, 00187 Roma, Italy; ¹⁸⁴INFN, Sezione di Trieste, Via Strada 6, 34100 Trieste, Italy; ¹⁸⁵INFN, Sezione di Genova, Via Dodecaneso 33, 16146 Genova, Italy; ¹⁸⁶INFN, Sezione di Pisa, Via F. Strozzi 2, 56127 Pisa, Italy; ¹⁸⁷INFN, Sezione di Roma, Via Ardeatina 546, 00187 Roma, Italy; ¹⁸⁸INFN, Sezione di Padova, Via Marzotto 1, 35100 Padova, Italy; ¹⁸⁹INFN, Sezione di Bologna, Via Irace 1, 40139 Bologna, Italy; ¹⁹⁰INFN, Sezione di Bari, Via Amendola 173, 70126 Bari, Italy; ¹⁹¹INFN, Sezione di Roma, Via Ardeatina 546, 00187 Roma, Italy; ¹⁹²INFN, Sezione di Trieste, Via Strada 6, 34100 Trieste, Italy; ¹⁹³INFN, Sezione di Genova, Via Dodecaneso 33, 16146 Genova, Italy; ¹⁹⁴INFN, Sezione di Pisa, Via F. Strozzi 2, 56127 Pisa, Italy; ¹⁹⁵INFN, Sezione di Roma, Via Ardeatina 546, 00187 Roma, Italy; ¹⁹⁶INFN, Sezione di Padova, Via Marzotto 1, 35100 Padova, Italy; ¹⁹⁷INFN, Sezione di Bologna, Via Irace 1, 40139 Bologna, Italy; ¹⁹⁸INFN, Sezione di Bari, Via Amendola 173, 70126 Bari, Italy; ¹⁹⁹INFN, Sezione di Roma, Via Ardeatina 546, 00187 Roma, Italy; ²⁰⁰INFN, Sezione di Trieste, Via Strada 6, 34100 Trieste, Italy; ²⁰¹INFN, Sezione di Genova, Via Dodecaneso 33, 16146 Genova, Italy; ²⁰²INFN, Sezione di Pisa, Via F. Strozzi 2, 56127 Pisa, Italy; ²⁰³INFN, Sezione di Roma, Via Ardeatina 546, 00187 Roma, Italy; ²⁰⁴INFN, Sezione di Padova, Via Marzotto 1, 35100 Padova, Italy; ²⁰⁵INFN, Sezione di Bologna, Via Irace 1, 40139 Bologna, Italy; ²⁰⁶INFN, Sezione di Bari, Via Amendola 173, 70126 Bari, Italy; ²⁰⁷INFN, Sezione di Roma, Via Ardeatina 546, 00187 Roma, Italy; ²⁰⁸INFN, Sezione di Trieste, Via Strada 6, 34100 Trieste, Italy; ²⁰⁹INFN, Sezione di Genova, Via Dodecaneso 33, 16146 Genova, Italy; ²¹⁰INFN, Sezione di Pisa, Via F. Strozzi 2, 56127 Pisa, Italy; ²¹¹INFN, Sezione di Roma, Via Ardeatina 546, 00187 Roma, Italy; ²¹²INFN, Sezione di Padova, Via Marzotto 1, 35100 Padova, Italy; ²¹³INFN, Sezione di Bologna, Via Irace 1, 40139 Bologna, Italy; ²¹⁴INFN, Sezione di Bari, Via Amendola 173, 70126 Bari, Italy; ²¹⁵INFN, Sezione di Roma, Via Ardeatina 546, 00187 Roma, Italy; ²¹⁶INFN, Sezione di Trieste, Via Strada 6, 34100 Trieste, Italy; ²¹⁷INFN, Sezione di Genova, Via Dodecaneso 33, 16146 Genova, Italy; ²¹⁸INFN, Sezione di Pisa, Via F. Strozzi 2, 56127 Pisa, Italy; ²¹⁹INFN, Sezione di Roma, Via Ardeatina 546, 00187 Roma, Italy; ²²⁰INFN, Sezione di Padova, Via Marzotto 1, 35100 Padova, Italy; ²²¹INFN, Sezione di Bologna, Via Irace 1, 40139 Bologna, Italy; ²²²INFN, Sezione di Bari, Via Amendola 173, 70126 Bari, Italy; ²²³INFN, Sezione di Roma, Via Ardeatina 546, 00187 Roma, Italy; ²²⁴INFN, Sezione di Trieste, Via Strada 6, 34100 Trieste, Italy; ²²⁵INFN, Sezione di Genova, Via Dodecaneso 33, 16146 Genova, Italy; ²²⁶INFN, Sezione di Pisa, Via F. Strozzi 2, 56127 Pisa, Italy; ²²⁷INFN, Sezione di Roma, Via Ardeatina 546, 00187 Roma, Italy; ²²⁸INFN, Sezione di Padova, Via Marzotto 1, 35100 Padova, Italy; ²²⁹INFN, Sezione di Bologna, Via Irace 1, 40139 Bologna, Italy; ²³⁰INFN, Sezione di Bari, Via Amendola 173, 70126 Bari, Italy; ²³¹INFN, Sezione di Roma, Via Ardeatina 546, 00187 Roma, Italy; ²³²INFN, Sezione di Trieste, Via Strada 6, 34100 Trieste, Italy; ²³³INFN, Sezione di Genova, Via Dodecaneso 33, 16146 Genova, Italy; ²³⁴INFN, Sezione di Pisa, Via F. Strozzi 2, 56127 Pisa, Italy; ²³⁵INFN, Sezione di Roma, Via Ardeatina 546, 00187 Roma, Italy; ²³⁶INFN, Sezione di Padova, Via Marzotto 1, 35100 Padova, Italy; ²³⁷INFN, Sezione di Bologna, Via Irace 1, 40139 Bologna, Italy; ²³⁸INFN, Sezione di Bari, Via Amendola 173, 70126 Bari, Italy; ²³⁹INFN, Sezione di Roma, Via Ardeatina 546, 00187 Roma, Italy; ²⁴⁰INFN, Sezione di Trieste, Via Strada 6, 34100 Trieste, Italy; ²⁴¹INFN, Sezione di Genova, Via Dodecaneso 33, 16146 Genova, Italy; ²⁴²INFN, Sezione di Pisa, Via F. Strozzi 2, 56127 Pisa, Italy; ²⁴³INFN, Sezione di Roma, Via Ardeatina 546, 00187 Roma, Italy; ²⁴⁴INFN, Sezione di Padova, Via Marzotto 1, 35100 Padova, Italy; ²⁴⁵INFN, Sezione di Bologna, Via Irace 1, 40139 Bologna, Italy; ²⁴⁶INFN, Sezione di Bari, Via Amendola 173, 70126 Bari, Italy; ²⁴⁷INFN, Sezione di Roma, Via Ardeatina 546, 00187 Roma, Italy; ²⁴⁸INFN, Sezione di Trieste, Via Strada 6, 34100 Trieste, Italy; ²⁴⁹INFN, Sezione di Genova, Via Dodecaneso 33, 16146 Genova, Italy; ²⁵⁰INFN, Sezione di Pisa, Via F. Strozzi 2, 56127 Pisa, Italy; ²⁵¹INFN, Sezione di Roma, Via Ardeatina 546, 00187 Roma, Italy; ²⁵²INFN, Sezione di Padova, Via Marzotto 1, 35100 Padova, Italy; ²⁵³INFN, Sezione di Bologna, Via Irace 1, 40139 Bologna, Italy; ²⁵⁴INFN, Sezione di Bari, Via Amendola 173, 70126 Bari, Italy; ²⁵⁵INFN, Sezione di Roma, Via Ardeatina 546, 00187 Roma, Italy; ²⁵⁶INFN, Sezione di Trieste, Via Strada 6, 34100 Trieste, Italy; ²⁵⁷INFN, Sezione di Genova, Via Dodecaneso 33, 16146 Genova, Italy; ²⁵⁸INFN, Sezione di Pisa, Via F. Strozzi 2, 56127 Pisa, Italy; ²⁵⁹INFN, Sezione di Roma, Via Ardeatina 546, 00187 Roma, Italy; ²⁶⁰INFN, Sezione di Padova, Via Marzotto 1, 35100 Padova, Italy; ²⁶¹INFN, Sezione di Bologna, Via Irace 1, 40139 Bologna, Italy; ²⁶²INFN, Sezione di Bari, Via Amendola 173, 70126 Bari, Italy; ²⁶³INFN, Sezione di Roma, Via Ardeatina 546, 00187 Roma, Italy; ²⁶⁴INFN, Sezione di Trieste, Via Strada 6, 34100 Trieste, Italy; ²⁶⁵INFN, Sezione di Genova, Via Dodecaneso 33, 16146 Genova, Italy; ²⁶⁶INFN, Sezione di Pisa, Via F. Strozzi 2, 56127 Pisa, Italy; ²⁶⁷INFN, Sezione di Roma, Via Ardeatina 546, 00187 Roma, Italy; ²⁶⁸INFN, Sezione di Padova, Via Marzotto 1, 35100 Padova, Italy; ²⁶⁹INFN, Sezione di Bologna, Via Irace 1, 40139 Bologna, Italy; ²⁷⁰INFN, Sezione di Bari, Via Amendola 173, 70126 Bari, Italy; ²⁷¹INFN, Sezione di Roma, Via Ardeatina 546, 00187 Roma, Italy; ²⁷²INFN, Sezione di Trieste, Via Strada 6, 34100 Trieste, Italy; ²⁷³INFN, Sezione di Genova, Via Dodecaneso 33, 16146 Genova, Italy; ²⁷⁴INFN, Sezione di Pisa, Via F. Strozzi 2, 56127 Pisa, Italy; ²⁷⁵INFN, Sezione di Roma, Via Ardeatina 546, 00187 Roma, Italy; ²⁷⁶INFN, Sezione di Padova, Via Marzotto 1, 35100 Padova, Italy; ²⁷⁷INFN, Sezione di Bologna, Via Irace 1, 40139 Bologna, Italy; ²⁷⁸INFN, Sezione di Bari, Via Amendola 173, 70126 Bari, Italy; ²⁷⁹INFN, Sezione di Roma, Via Ardeatina 546, 00187 Roma, Italy; ²⁸⁰INFN, Sezione di Trieste, Via Strada 6, 34100 Trieste, Italy; ²⁸¹INFN, Sezione di Genova, Via Dodecaneso 33, 16146 Genova, Italy; ²⁸²INFN, Sezione di Pisa, Via F. Strozzi 2, 56127 Pisa, Italy; ²⁸³INFN, Sezione di Roma, Via Ardeatina 546, 00187 Roma, Italy; ²⁸⁴INFN, Sezione di Padova, Via Marzotto 1, 35100 Padova, Italy; ²⁸⁵INFN, Sezione di Bologna, Via Irace 1, 40139 Bologna, Italy; ²⁸⁶INFN, Sezione di Bari

In August 2008, a man took a photograph somewhere in Stockholm . . .



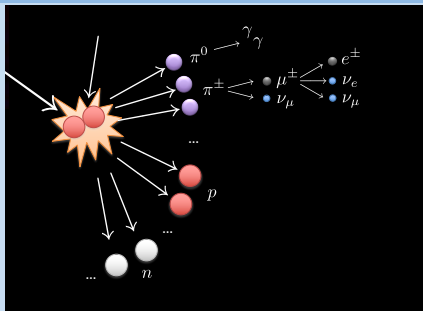
Secondary



- e^+ from spallation of cosmic ray nuclei on gas
 - Energy losses make e^\pm spectrum softer
- Positron fraction $e^+/(e^+ + e^-)$ should decrease with energy

Positron excess

Secondary



- e^+ from spallation of cosmic ray nuclei on gas
 - Energy losses make e^\pm spectrum softer
- Positron fraction $e^+/(e^+ + e^-)$ should decrease with energy

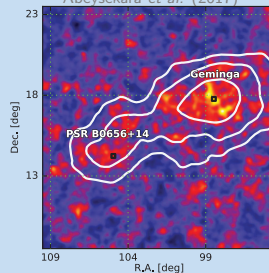
Dark matter



Now strongly constrained by γ -rays, \bar{p} , CMB!

Pulsars/PWNe

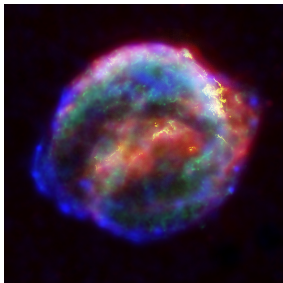
Abeyssekara et al. (2017)



Must be contributing at some level?!

Secondaries from the source?

Common belief: secondaries from propagation dominate since the grammage in the ISM is larger than in the source



$$\begin{aligned}\langle \tau_{\text{src}} \rangle &\lesssim \tau_{\text{SNR}} \approx 10^{4 \dots 5} \text{ yr} \\ n_{\text{src}} &\lesssim 10 \text{ cm}^{-3} \\ \Rightarrow X_{\text{src}} &\approx 0.2 \text{ g cm}^{-2}\end{aligned}$$



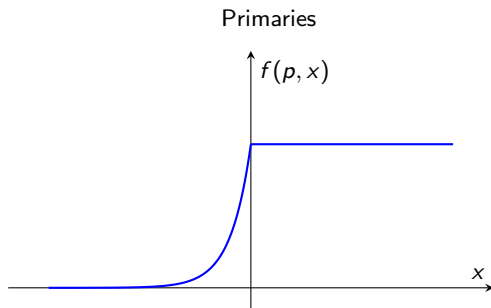
$$\begin{aligned}\langle \tau_{\text{ISM}} \rangle &\sim \tau_{\text{esc}} \approx 10^7 \text{ yr} \\ n_{\text{ISM}} &\approx 0.1 \text{ cm}^{-3} \\ \Rightarrow X_{\text{ISM}} &\approx \text{few g cm}^{-2}\end{aligned}$$

However, secondaries from source can have a harder spectrum!

Diffusive shock acceleration with secondaries

Blasi (2009); Blasi & Serpico (2009); Mertsch & Sarkar (2009); Ahlers *et al.* (2010); Tomassetti & Donato (2012); Cholis & Hooper (2012); Mertsch & Sarkar (2014); Cholis *et al.* (2017); Mertsch, Vittino, Sarkar (2021); Kawanaka & Lee (2021)

Spatial distribution



Spectral distribution

$$f(x = 0, p) \propto p^{-\gamma} \quad \text{with } \gamma = \frac{3U_1}{U_1 - U_2}$$

$\Rightarrow E^{-2}$ spectrum

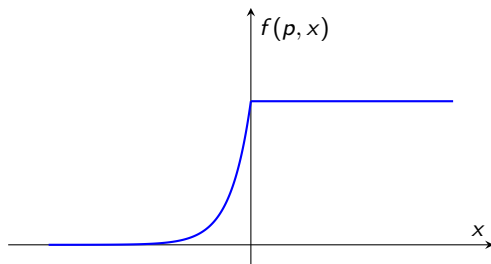
Diffusive shock acceleration with secondaries

Blasi (2009); Blasi & Serpico (2009); Mertsch & Sarkar (2009); Ahlers *et al.* (2010); Tomassetti & Donato (2012); Cholis & Hooper (2012); Mertsch & Sarkar (2014); Cholis *et al.* (2017); Mertsch, Vittino, Sarkar (2021); Kawanaka & Lee (2021)

Spatial distribution

Spectral distribution

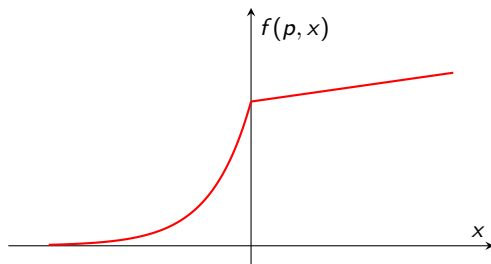
Primaries



$$f(x = 0, p) \propto p^{-\gamma} \quad \text{with } \gamma = \frac{3U_1}{U_1 - U_2}$$

$\Rightarrow E^{-2}$ spectrum

Secondaries



$$f(x = 0, p) \propto p^{-\gamma+1}$$

\Rightarrow Harder secondary spectrum

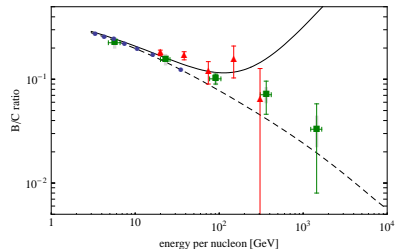
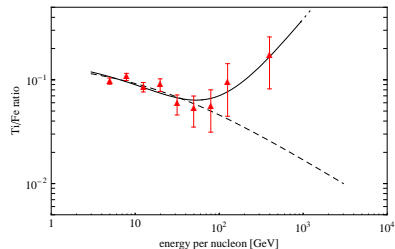
Secondary nuclei as a check

Mertsch & Sarkar, PRL 103 (2009) 081104

On 17.03.09 14:47, Subir Sarkar wrote:

However one can then ask why other secondary/primary ratios e.g. Li, Be, B/C, N, O in fact decrease with energy [...]. So my question would be: if the same SNRs are also accelerating cosmic ray nuclei then is the expected secondary/primary ratio (according to Blasi's calculation) consistent with the observations?

Tuned to ATIC data:



PRL 103, 081104 (2009)

PHYSICAL REVIEW LETTERS

week ending
21 AUGUST 2009

Testing Astrophysical Models for the PAMELA Positron Excess with Cosmic Ray Nuclei

Philipp Mertsch and Subir Sarkar

Rudolf Peierls Centre for Theoretical Physics, University of Oxford, Oxford OX1 3NP, United Kingdom
(Received 21 May 2009; revised manuscript received 9 July 2009; published 21 August 2009)

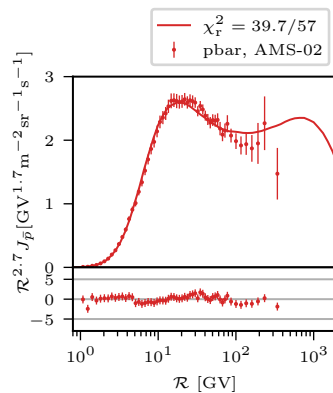
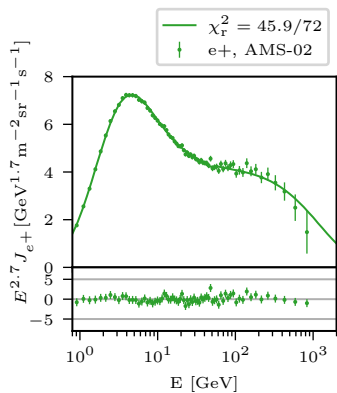
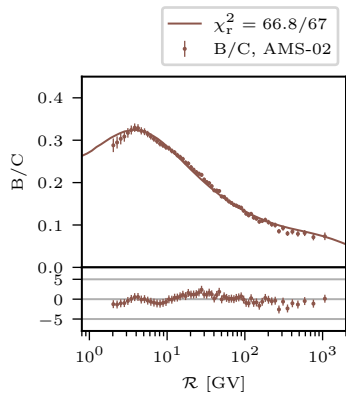
The excess in the positron fraction measured by PAMELA has been interpreted as due to annihilation or decay of dark matter in the Galaxy. More prosaically it has been ascribed to direct production of positrons by nearby pulsars or due to pion production during diffusive shock acceleration of hadronic cosmic rays in nearby sources. We point out that measurements of secondary cosmic ray nuclei can discriminate between these possibilities. New data on the titanium-to-iron ratio support the hadronic source model above and enable a prediction for the boron-to-carbon ratio at energies above 100 GeV.

DOI: 10.1103/PhysRevLett.103.081104

PACS numbers: 98.70.Sa, 96.50.sb, 98.58.Mj

A recent update

Mertsch, Vittino, Sarkar, PRD 104 (2021) 103029

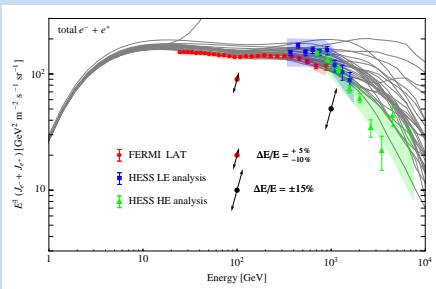


Further improvements

Ahlers, Mertsch, Sarkar (2009)

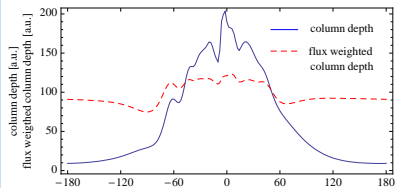
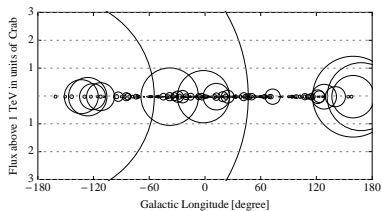
Stochasticity

- e^\pm suffer severe energy losses
- Sensitivity to nearby sources
- Predictions are probabilistic



Gamma-rays

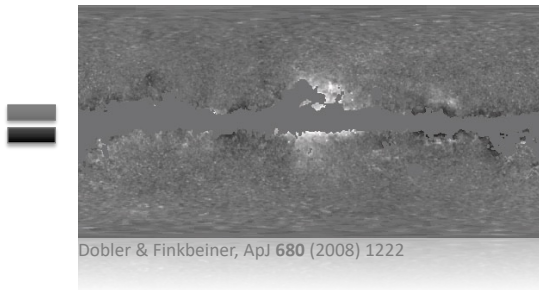
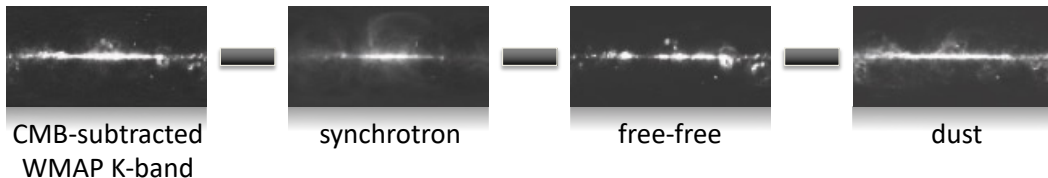
- If $\text{CR} + \text{gas} \rightarrow e^\pm + \dots$,
then also $\text{CR} + \text{gas} \rightarrow \gamma + \gamma$



Exposure



Claim by Finkbeiner (2004)

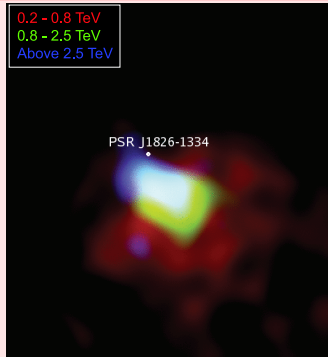


1. morphology: roughly spherical
2. power: few kJy sr^{-1}
3. spectrum: harder than usual synchrotron

Is the WMAP haze real?

Template subtraction assumes
that morphology
is energy-independent

Counter example

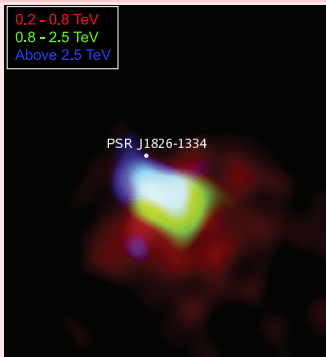


Funk *et al.*, ICRC proceedings (2007)

Is the WMAP haze real?

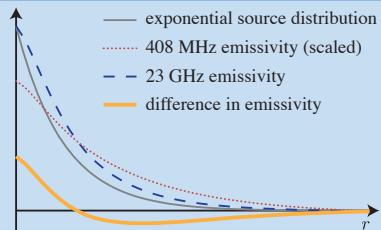
Template subtraction assumes
that morphology
is energy-independent

Counter example



Funk *et al.*, ICRC proceedings (2007)

Radial distribution of emissivity



Agrees with WMAP haze in ...

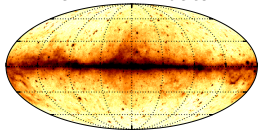
- Morphology
- Normalisation
- Spectrum

Mertsch & Sarkar, JCAP 10 (2010) 019

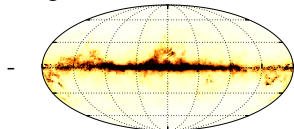
The Fermi bubbles

Su et al. (2010); Ackermann et al. (2013)

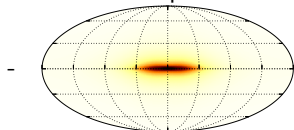
Fermi-LAT data



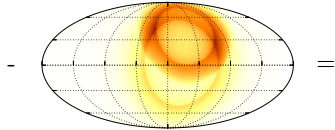
gas-correlated emission



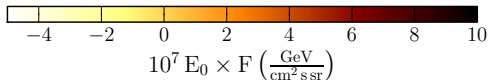
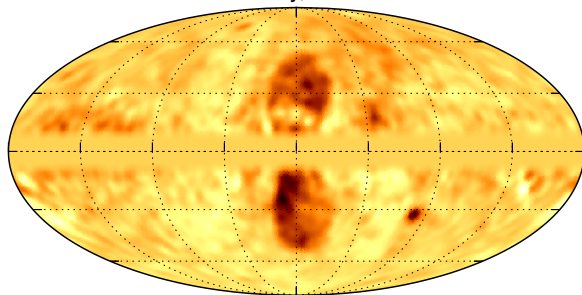
Inverse Compton model



some other stuff



Residual intensity, $E = 3 - 10$ GeV

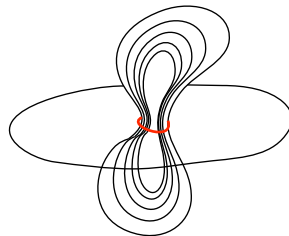
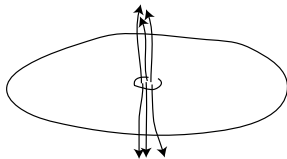


- Hard spectrum
- Sharp edges
- No spectral variation

Fermi bubbles

Star formation activity

Crocker & Aharonian (2011)



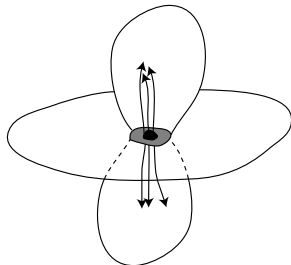
Tidal disruption events

Cheng *et al.* (2011)

Previous AGN phase

Guo & Mathews, ApJ 756 (2012) 181;

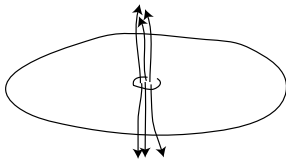
Yang *et al.*, ApJ 761 (2012) 185



Fermi bubbles

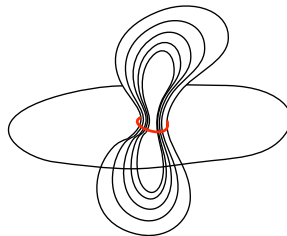
Star formation activity

Crocker & Aharonian (2011)



Tidal disruption events

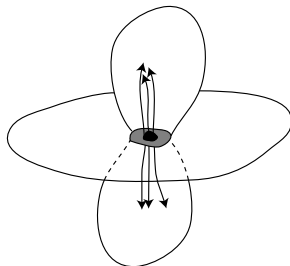
Cheng *et al.* (2011)



Previous AGN phase

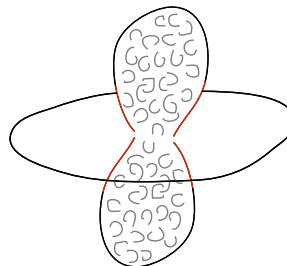
Guo & Mathews, ApJ 756 (2012) 181;

Yang *et al.*, ApJ 761 (2012) 185



Large-scale turbulence

Mertsch & Sarkar (2011)



Mon. Not. R. astr. Soc. (1984) **207**, 745–775

The evolution of supernova remnants as radio sources

Ramanath Cowsik and Subir Sarkar* *Tata Institute of
Fundamental Research, Homi Bhabha Road, Bombay 400005, India*

Received 1983 August 10; in original form 1982 July 9

Summary. The acceleration of relativistic electrons by hydromagnetic turbulence in shell-type supernova remnants (SNRs) is examined in relation to their structural development through interaction with the interstellar medium. The transport equation governing the energy spectrum of the electrons is analytically solved, enabling study of the evolution of their synchrotron radio emission.

The sudden emergence of SNRs as long-lived radio sources, several decades after the supernova event, is then explained. Their subsequent radio evolution, with spectral changes and structural details as exemplified by the young remnant Cassiopeia A, follows naturally. The absence of younger radio remnants in the Galaxy implies a supernova rate lower than that inferred from extragalactic observations. The collective properties of galactic SNRs suggest a mild acceleration of electrons throughout the adiabatic phase of evolution. SNRs may thus contribute significantly to cosmic-ray electrons in the Galaxy.

1 Introduction

While thermal emission from SNRs at optical and X-ray wavelengths is reasonably well understood in terms of shock wave propagation in the interstellar medium (see Chevalier 1977a; Raymond 1979; Itoh 1982), the situation regarding non-thermal radio emission is less satisfactory. In remnants which resemble the Crab Nebula, a central pulsar may generate the necessary relativistic electrons and magnetic field (e.g. Weiler & Panagia 1978). However, the majority of SNRs are shell-like, suggestive of interaction with the interstellar medium. In old remnants this presumably happens through compression of the interstellar magnetic field together with cosmic-ray electrons, in the dense cooling regions behind the associated slow, radiative shock waves (e.g. Duin & van der Laan 1975). An alternative mechanism is required for young remnants with adiabatically propagating fast shocks, which cannot compress by more than a factor of 4.

*Presently visiting Department of Astrophysics, University of Oxford, South Parks Road, Oxford OX1 3JQ.

2nd order Fermi acceleration

1984MNRAS...207...745C

Mon. Not. R. astr. Soc. (1984) **207**, 745–775

The evolution of supernova remnants as radio sources

Ramanath Cowsik and Subir Sarkar* *Tata Institute of Fundamental Research, Homi Bhabha Road, Bombay 400005, India*

Received 1983 August 10; in original form 1982 July 9

Summary. The acceleration of relativistic electrons by hydromagnetic turbulence in shell-type supernova remnants (SNRs) is examined in relation to their structural development through interaction with the interstellar medium. The transport equation governing the energy spectrum of the electrons is analytically solved, enabling study of the evolution of their synchrotron radio emission.

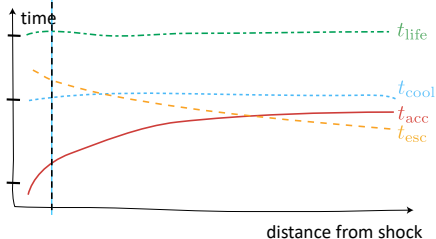
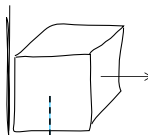
The sudden emergence of SNRs as long-lived radio sources, several decades after the supernova event, is then explained. Their subsequent radio evolution, with spectral changes and structural details as exemplified by the young remnant Cassiopeia A, follows naturally. The absence of younger radio remnants in the Galaxy implies a supernova rate lower than that inferred from extragalactic observations. The collective properties of galactic SNRs suggest a mild acceleration of electrons throughout the adiabatic phase of evolution. SNRs may thus contribute significantly to cosmic-ray electrons in the Galaxy.

1 Introduction

While thermal emission from SNRs at optical and X-ray wavelengths is reasonably well understood in terms of shock wave propagation in the interstellar medium (see Chevalier 1977a; Raymond 1979; Itoh 1982), the situation regarding non-thermal radio emission is less satisfactory. In remnants which resemble the Crab Nebula, a central pulsar may generate the necessary relativistic electrons and magnetic field (e.g. Weiler & Panagia 1978). However, the majority of SNRs are shell-like, suggestive of interaction with the interstellar medium. In old remnants this presumably happens through compression of the interstellar magnetic field together with cosmic-ray electrons, in the dense cooling regions behind the associated slow, radiative shock waves (e.g. Duijn & van der Laan 1975). An alternative mechanism is required for young remnants with adiabatically propagating fast shocks, which cannot compress by more than a factor of 4.

*Presently visiting Department of Astrophysics, University of Oxford, South Parks Road, Oxford OX1 3JQ.

shock



2nd order Fermi acceleration

1984MNRAS...134C

Mon. Not. R. astr. Soc. (1984) **207**, 745–775

The evolution of supernova remnants as radio sources

Ramanath Cowsik and Subir Sarkar* *Tata Institute of Fundamental Research, Homi Bhabha Road, Bombay 400005, India*

Received 1983 August 10; in original form 1982 July 9

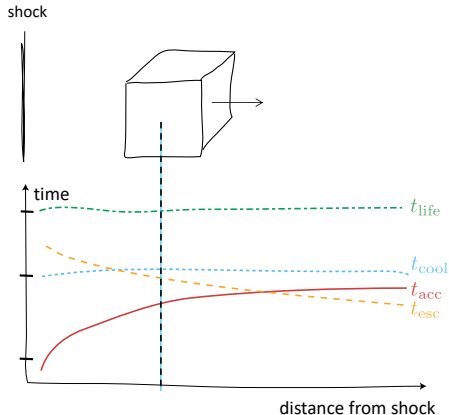
Summary. The acceleration of relativistic electrons by hydromagnetic turbulence in shell-type supernova remnants (SNRs) is examined in relation to their structural development through interaction with the interstellar medium. The transport equation governing the energy spectrum of the electrons is analytically solved, enabling study of the evolution of their synchrotron radio emission.

The sudden emergence of SNRs as long-lived radio sources, several decades after the supernova event, is then explained. Their subsequent radio evolution, with spectral changes and structural details as exemplified by the young remnant Cassiopeia A, follows naturally. The absence of younger radio remnants in the Galaxy implies a supernova rate lower than that inferred from extragalactic observations. The collective properties of galactic SNRs suggest a mild acceleration of electrons throughout the adiabatic phase of evolution. SNRs may thus contribute significantly to cosmic-ray electrons in the Galaxy.

1 Introduction

While thermal emission from SNRs at optical and X-ray wavelengths is reasonably well understood in terms of shock wave propagation in the interstellar medium (see Chevalier 1977a; Raymond 1979; Itoh 1982), the situation regarding non-thermal radio emission is less satisfactory. In remnants which resemble the Crab Nebula, a central pulsar may generate the necessary relativistic electrons and magnetic field (e.g. Weiler & Panagia 1978). However, the majority of SNRs are shell-like, suggestive of interaction with the interstellar medium. In old remnants this presumably happens through compression of the interstellar magnetic field together with cosmic-ray electrons, in the dense cooling regions behind the associated slow, radiative shock waves (e.g. Duin & van der Laan 1975). An alternative mechanism is required for young remnants with adiabatically propagating fast shocks, which cannot compress by more than a factor of 4.

*Presently visiting Department of Astrophysics, University of Oxford, South Parks Road, Oxford OX1 3RQ.



2nd order Fermi acceleration

1984MNRAS...207...745C

Mon. Not. R. astr. Soc. (1984) **207**, 745–775

The evolution of supernova remnants as radio sources

Ramanath Cowsik and Subir Sarkar* *Tata Institute of Fundamental Research, Homi Bhabha Road, Bombay 400005, India*

Received 1983 August 10; in original form 1982 July 9

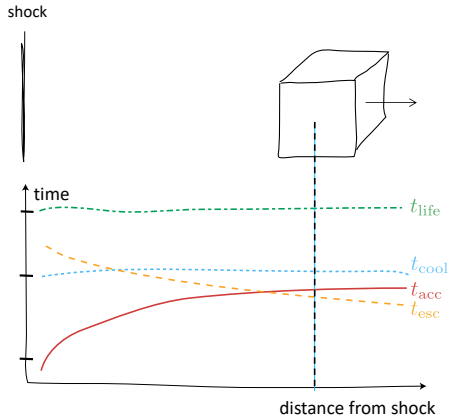
Summary. The acceleration of relativistic electrons by hydromagnetic turbulence in shell-type supernova remnants (SNRs) is examined in relation to their structural development through interaction with the interstellar medium. The transport equation governing the energy spectrum of the electrons is analytically solved, enabling study of the evolution of their synchrotron radio emission.

The sudden emergence of SNRs as long-lived radio sources, several decades after the supernova event, is then explained. Their subsequent radio evolution, with spectral changes and structural details as exemplified by the young remnant Cassiopeia A, follows naturally. The absence of younger radio remnants in the Galaxy implies a supernova rate lower than that inferred from extragalactic observations. The collective properties of galactic SNRs suggest a mild acceleration of electrons throughout the adiabatic phase of evolution. SNRs may thus contribute significantly to cosmic-ray electrons in the Galaxy.

1 Introduction

While thermal emission from SNRs at optical and X-ray wavelengths is reasonably well understood in terms of shock wave propagation in the interstellar medium (see Chevalier 1977a; Raymond 1979; Itoh 1982), the situation regarding non-thermal radio emission is less satisfactory. In remnants which resemble the Crab Nebula, a central pulsar may generate the necessary relativistic electrons and magnetic field (e.g. Weiler & Panagia 1978). However, the majority of SNRs are shell-like, suggestive of interaction with the interstellar medium. In old remnants this presumably happens through compression of the interstellar magnetic field together with cosmic-ray electrons, in the dense cooling regions behind the associated slow, radiative shock waves (e.g. Duijn & van der Laan 1975). An alternative mechanism is required for young remnants with adiabatically propagating fast shocks, which cannot compress by more than a factor of 4.

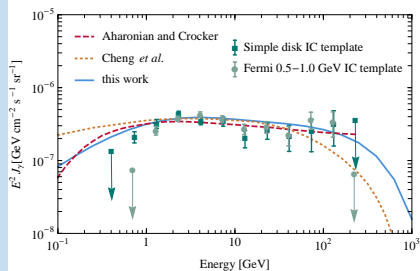
*Presently visiting Department of Astrophysics, University of Oxford, South Parks Road, Oxford OX1 3RO.



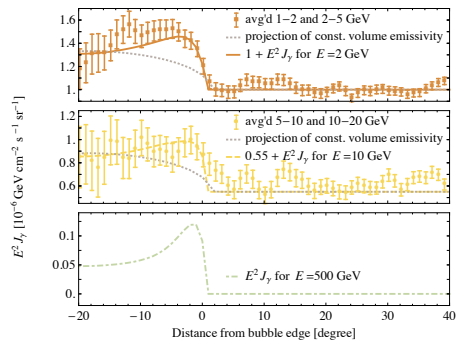
Fermi bubbles

Mertsch & Sarkar (2011)

Spectrum



Profile

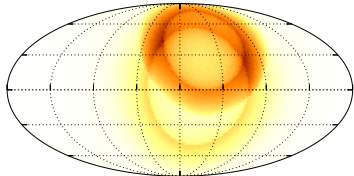


The elephant in the room

Banksy



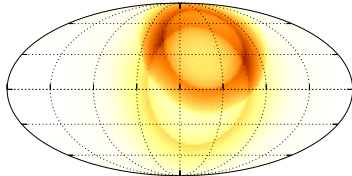
some other stuff



The elephant in the room



some other stuff



UDHARWAL, 1997, 97

Mon. Not. R. astr. Soc. (1982) 199, 97–108

Does the galactic synchrotron radio background originate in old supernova remnants?

Subir Sarkar *Tata Institute of Fundamental Research, Homi Bhabha Road, Bombay 400005, India*

Received 1981 August 3; in original form 1981 May 7

Summary. Observations of the galactic synchrotron radio background indicate that the emission arises in localized regions of high emissivity. Various lines of evidence suggest that these are the radiative shells of old supernova remnants in which the synchrotron emissivity is enhanced due to compression of the interstellar magnetic field along with the correlated increase in the energy density of cosmic ray electrons. This possibility is consistent with recent observations of the interstellar medium that imply the presence of a large amount of hot, low density gas in the galaxy. In such a medium supernova remnants would expand to large radii before becoming radiative.

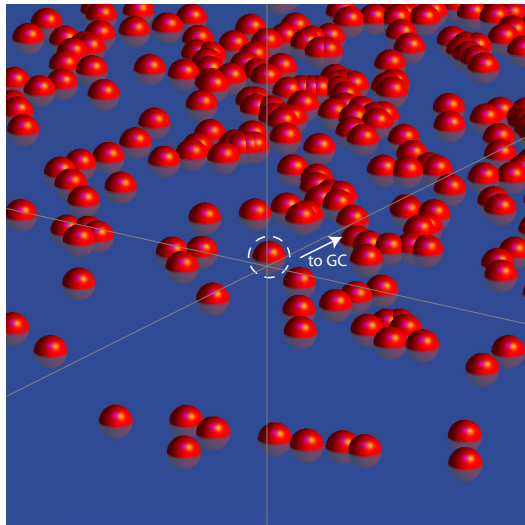
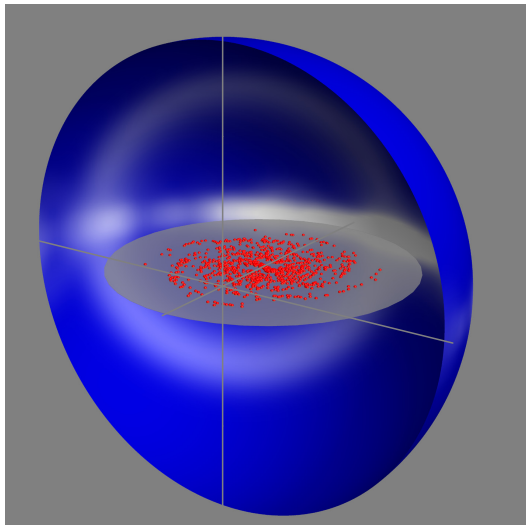
The intensity of the background can then be understood without needing to evoke higher magnetic fields or cosmic ray electron fluxes than are obtained from other observations. In this picture, the fluctuating component of the galactic magnetic field arises from the distortion of the regular field by the shells.

Other explanations for the origin of the background are briefly discussed. This result casts doubt on the existence of large-scale cosmic ray gradients inferred from galactic gamma ray observations.

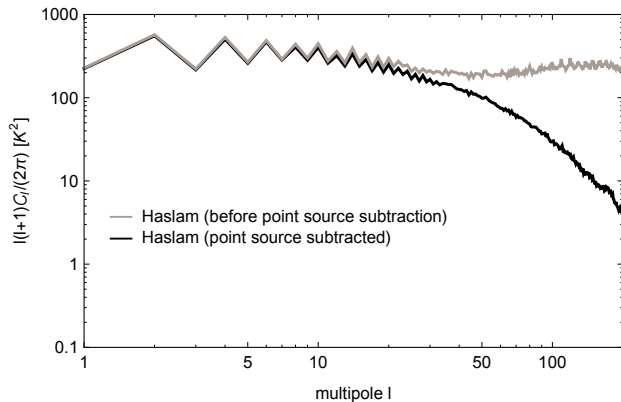
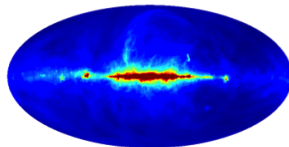
1 Introduction

The 'standard' interpretation of the diffuse galactic synchrotron radio background as due to cosmic ray electrons radiating uniformly throughout the Galaxy leads to the well-known discrepancy between the observed and calculated strength of the emission (*cf.* Daniel & Stephens 1975). To reconcile them it appears necessary to postulate either much higher electron fluxes elsewhere in the Galaxy than observed locally (Seri & Wolter 1971) or much higher magnetic fields than are obtained from other observations (e.g. Badhwar, Daniel & Stephens 1977). As a conceptual way out of this difficulty, Cowsik & Mitteldorf (1974) have suggested that if fluctuations in the galactic magnetic field arise from compressions of the average fields by motions of the interstellar gas, then betatron processes induce a correlated increase of the relativistic electron energy density in the high field regions. The enhanced synchrotron emission from such regions then raises the average interstellar emissivity to match the observations.

Where is Loop I?

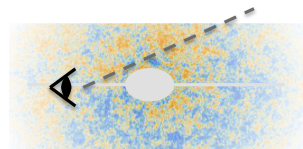
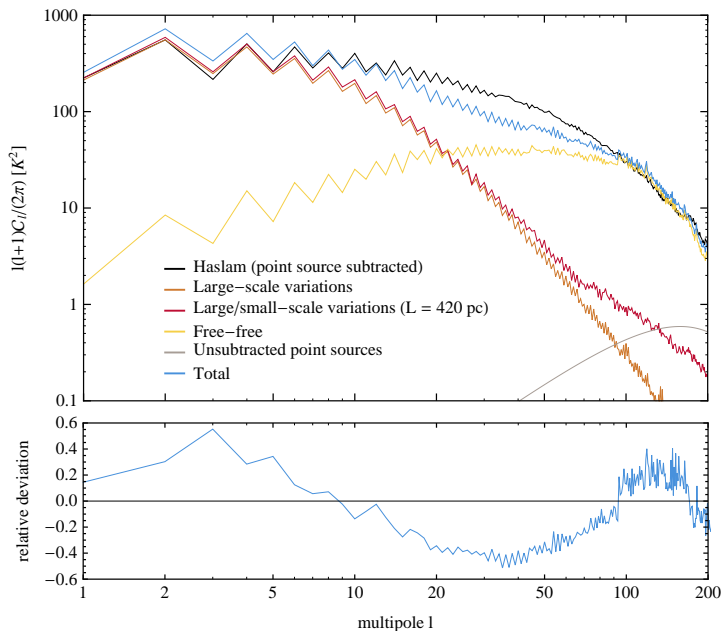


Are the $\mathcal{O}(1000)$ other old supernova remnants visible?



- 1 Even/odd structure \Leftrightarrow symmetry of Galactic disk
- 2 On large scales: less fluctuations
- 3 On large scales: power-law behaviour

GALPROP + turbulence + free-free + pt. sources



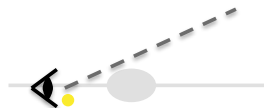
- Synchrotron from turbulent **B-field**
- Free-free: thermal bremsstrahlung
- Unsubtracted point sources: shot noise

Deficit in angular power spectrum

Modelling shells in harmonic space

Assumption: flux from one shell factorises into angular part and frequency part,

$$J_{\text{shell},i}(\nu, \ell, b) = \varepsilon_i(\nu) g_i(\ell, b)$$



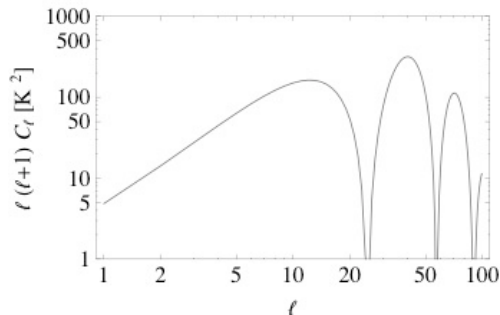
Frequency part $\varepsilon_i(\nu)$:

- Magnetic field compressed in SNR shell
- Electrons get betatron accelerated
- Emissivity increased with respect to ISM

Angular part $g_i(\ell, b)$:

Assume constant emissivity in thin shell:

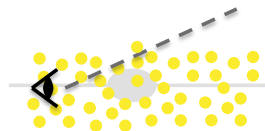
$$a_{\ell m}^{(i)'} \sim \varepsilon_i(\nu) \int_{-1}^1 dz' P_{\ell}(z') g_i(z')$$



Modelling shells in harmonic space

Assumption: flux from one shell factorises into angular part and frequency part,

$$J_{\text{shell},i}(\nu, \ell, b) = \varepsilon_i(\nu) g_i(\ell, b)$$



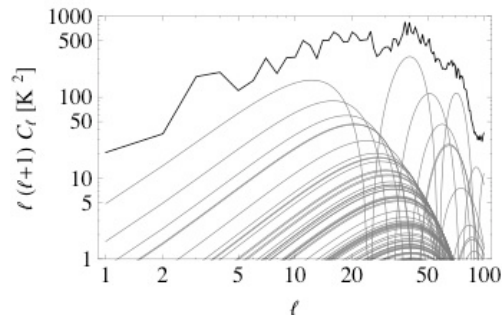
Frequency part $\varepsilon_i(\nu)$:

- Magnetic field compressed in SNR shell
- Electrons get betatron accelerated
- Emissivity increased with respect to ISM

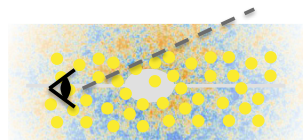
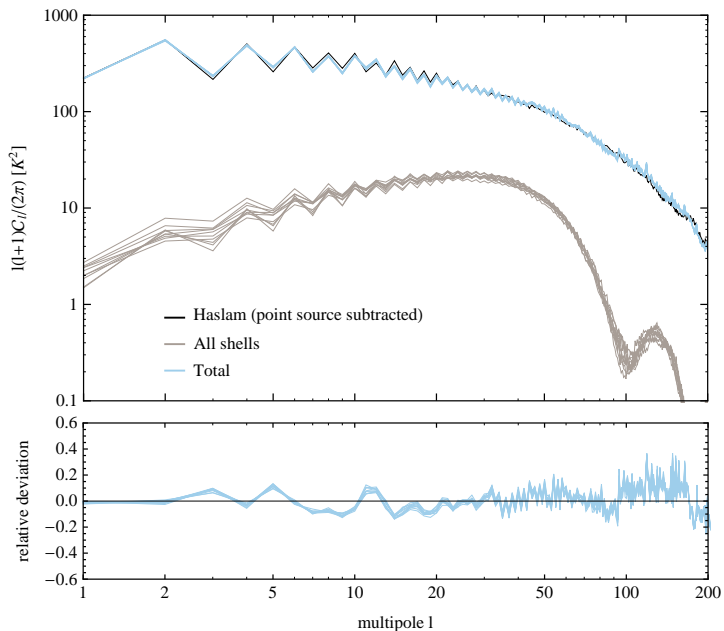
Angular part $g_i(\ell, b)$:

Assume constant emissivity in thin shell:

$$a_{\ell m}^{(i)'} \sim \varepsilon_i(\nu) \int_{-1}^1 dz' P_{\ell}(z') g_i(z')$$



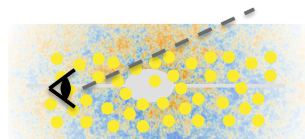
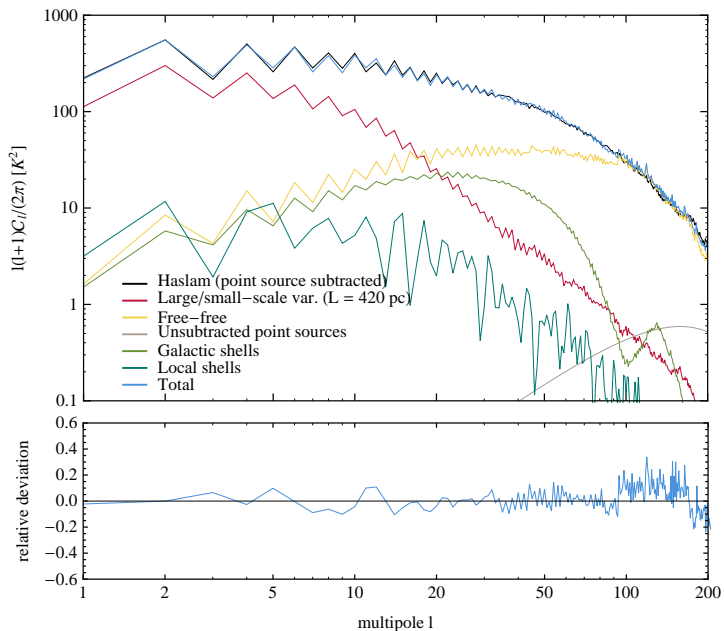
GALPROP + turbulence + free-free + pt. sources + shells



- Synchrotron from turbulent **B-field**
- Free-free: thermal bremsstrahlung
- Unsubtracted point sources: shot noise
- $\mathcal{O}(1000)$ shells of old supernova remnants

Contribute on exactly the right angular scales

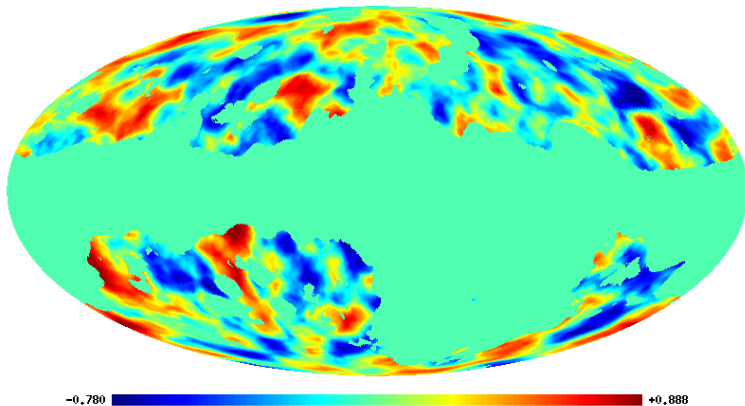
GALPROP + turbulence + free-free + pt. sources + shells



- Synchrotron from turbulent **B-field**
- Free-free: thermal bremsstrahlung
- Unsubtracted point sources: shot noise
- $\mathcal{O}(1000)$ shells of old supernova remnants

Contribute on exactly the right angular scales

CMB contamination at high latitudes?

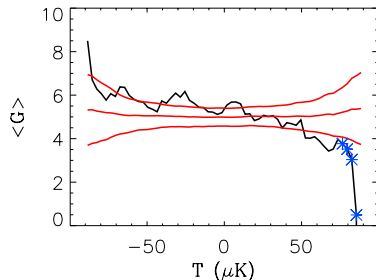
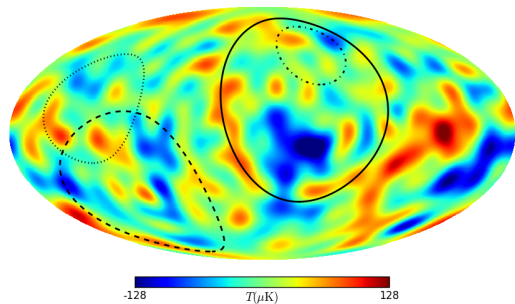


- Correlation between Faraday depth and WMAP7 ILC
- MC simulations: standard deviation of correlation anomalous with $p\text{-value} < 5 \times 10^{-4}$

Hansen *et al.*, MNRAS 426 (2012) 57; Dineen & Coles, MNRAS 347 (2004) 52

Anomalies in ILC9 ($\ell \leq 20$)

Liu, Mertsch & Sarkar, ApJL 789 (2014) 29



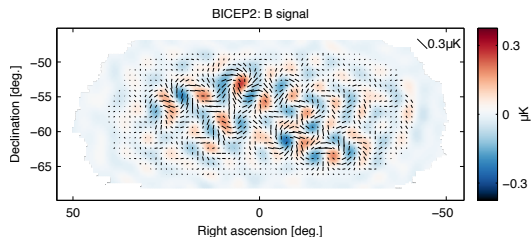
- Black: Loops I-IV Berkhuijsen, Salter (1971)
- Average temperature and skewness: p-values at 10^{-2} level

- Distance of clusters from ring: p-value 10^{-4}

In early March 2014, a man knocked on a door somewhere in Silicon Valley ...



In early March 2014, a man knocked on a door somewhere in Silicon Valley ...

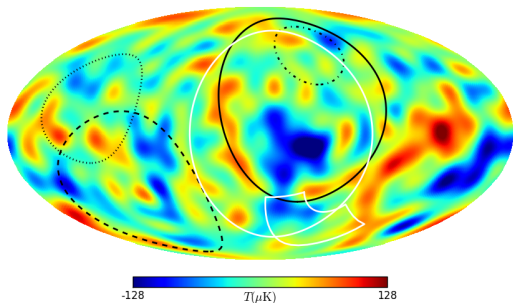


Ade *et al.*, PRL 112 (2014) 241101

- Observation of B-mode polarisation of the CMB, $r = 0.2$ at $\gtrsim 5\sigma$ significance
- Evidence for cosmological inflation
- Foreground contamination excluded

Anomalies in ILC9 ($\ell \leq 20$)

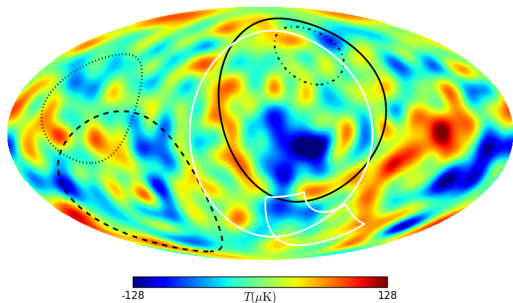
Liu, Mertsch & Sarkar, ApJL 789 (2014) 29



- Black: Loops I-IV Berkhuijsen, Salter (1971)
- White: S1 Wolleben (2007) and BICEP2 field

Anomalies in ILC9 ($\ell \leq 20$)

Liu, Mertsch & Sarkar, ApJL 789 (2014) 29



Added an innocent comment to last paragraph:

- Wolleben loop S1 goes through BICEP field
- Radio loops usually not modelled
- This can affect the significance

- Black: Loops I-IV Berkhuysen, Salter (1971)
- White: S1 Wolleben (2007) and BICEP2 field

10 minutes in the (cosmo) spot light

- Some coverage by the Washington Post, New Scientist, Physics World, Die Zeit
- From the facebook thread “Live Discussion of BICEP Press Conference”:

 **Scott Dodelson**
Admin · 8 April 2014 · 🌐

Any thoughts about <http://arxiv.org/abs/1404.1899?>

 ARXIV.ORG
[1404.1899] Fingerprints of Galactic Loop I on the Cosmic Microwave Background

👍 27 💬 38 comments

👍 Like 💬 Comment 📧 Send

These guys need to analyze the foreground cleaned Planck CMB maps, not just the WMAP ILC map. The spurs are known to have steeper spectral indices than the average synchrotron, and the ILC method cannot account for this. However, other methods do, so it's critical to check that this isn't just an ILC issue. Quite surprised they didn't already present those results, actually...

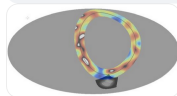
Like 9 y 👍 3

I strongly dislike papers that throw out a line at the end like: "this is a potential systematic for observation X or experiment Y" with zero quantitative backing to that statement.

Oh, and the 150x100 correlation in the bicep2 paper is with bicep1 data; the correlation with keck is all at 150.

Like 9 y 👍 5

Things you do when you're in an all-day meeting: I grabbed Fig. 24, bottom left panel, from the BICEP2 instrument paper, reprojected it from Cartesian projection to Healpix pixelization, and overlaid it on Fig. 2 from 1404.1899. The full BICEP2 region just barely touches the loop, and the main, high-N_obs region is never less than 10 degrees away. Put more simply, Loop 1 extends to galactic latitude of about -40, while the important BICEP2 region is never higher than -50.



Like 9 y 👍 20

 **Arman Shflu**
Philipp Mertsch

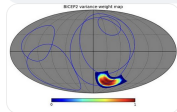
Like 9 y

 **Philipp Mertsch**
Sorry, just catching up with this now:

Hans Kristian, we have studied the Planck SMICA map, also the map by Starck et al. (arXiv:1401.6016 [astro-ph.CO]), but this part of the analysis didn't make it into the final paper. I'm confident that whoever repeats our analysis with those maps will find largely the same results.

Tom, please note that we did not claim a systematic in the BICEP2 measurement, but instead pointed out that the foreground models they refer to lack an ingredient that we know must be there: radio loops. If it turns out it's negligible: fine, but don't you think it's worth checking?

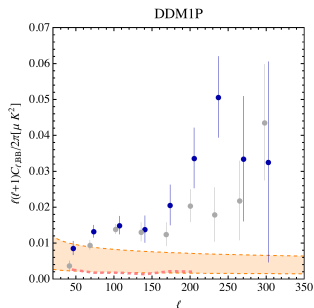
Finally, thanks, Dave and Colin, for emphasising that in our conclusion we were mainly referring to Wolleben's "New Loop". It is shown together with Loops I-IV (as defined by Berkhuijsen et al. in the early 70ies) and the variance-weighted BICEP2 field in this figure. The upper large loop roughly around the Galactic centre is Loop I, the lower one (cutting right through the BICEP2 field) is Wolleben's "New Loop".



Like 9 y 👍 4

How this got resolved

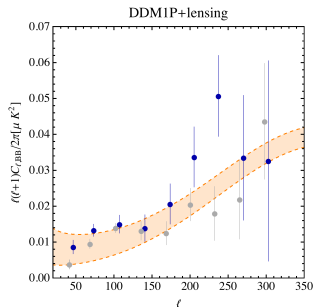
- BICEP2 used some preliminary Planck polarisation fractions for foreground model
- Some ambiguity as to zero-levels and cosmic infrared background (CIB)
- Likely some underestimate of foregrounds



R. Flauger, "Simplicity" workshop (2014)

How this got resolved

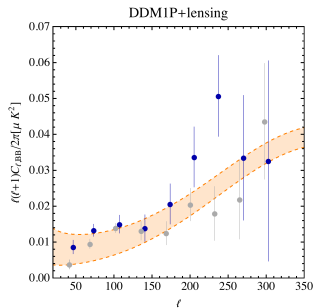
- BICEP2 used some preliminary Planck polarisation fractions for foreground model
- Some ambiguity as to zero-levels and cosmic infrared background (CIB)
- Likely some underestimate of foregrounds



R. Flauger, "Simplicity" workshop (2014)

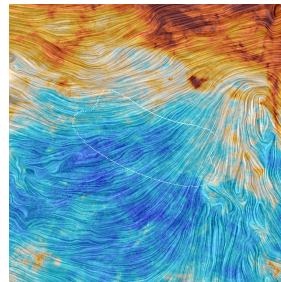
How this got resolved

- BICEP2 used some preliminary Planck polarisation fractions for foreground model
- Some ambiguity as to zero-levels and cosmic infrared background (CIB)
- Likely some underestimate of foregrounds

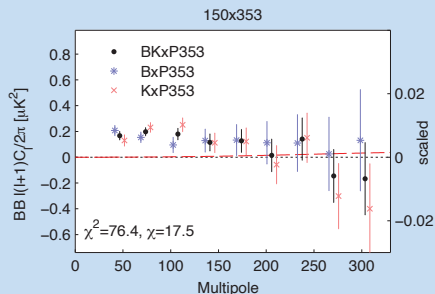


R. Flauger, "Simplicity" workshop (2014)

Planck view of
BICEP2 field:



Joint Planck-BICEP2 analysis



" $r < 0.12$ at 95% confidence"

Thank you, Subir,

- for giving me the freedom to choose my own projects,
- for giving me exposure with the community,
- for instilling critical thinking in me!

Thank you, Subir,

- for giving me the freedom to choose my own projects,
- for giving me exposure with the community,
- for instilling critical thinking in me!



Thank you, Subir,

- for giving me the freedom to choose my own projects,
- for giving me exposure with the community,
- for instilling critical thinking in me!

